Draft version April 25, 2025
Typeset using LaTeX **twocolumn** style in AASTeX631

The First Photometric Evidence of a Transient/Variable Source at $z > 5$ with *JWST*

Christa DeCoursey,[1] Eiichi Egami,[1] Fengwu Sun,[2] Arshia Akhtarkavan,[1] Rachana Bhatawdekar,[3] Andrew J. Bunker,[4] David A. Coulter,[5] Michael Engesser,[5] Ori D. Fox,[5] Sebastian Gomez,[5] Kohei Inayoshi,[6] Benjamin D. Johnson,[2] Mitchell Karmen,[7] Conor Larison,[5] Xiaojing Lin,[8,1] Jianwei Lyu,[1] Seppo Mattila,[9,10] Takashi J. Moriya,[11,12,13] Justin D. R. Pierel,[5,*] Dávid Puskás,[14,15] Armin Rest,[5,7] George H. Rieke,[1] Brant Robertson,[16] Sepehr Salamat,[1] Louis-Gregory Strolger,[5] Sandro Tacchella,[14,15] Christian Vassallo,[9] Christina C. Williams,[17] Yossef Zenati,[7,5,18] and Junyu Zhang[1]

[1]*Steward Observatory, University of Arizona, 933 N. Cherry Ave, Tucson, AZ 85721, USA*
[2]*Center for Astrophysics | Harvard & Smithsonian, 60 Garden St., Cambridge MA 02138 USA*
[3]*European Space Agency (ESA), European Space Astronomy Centre (ESAC), Camino Bajo del Castillo s/n, 28692 Villanueva de la Cañada, Madrid, Spain*
[4]*Department of Physics, University of Oxford, Denys Wilkinson Building, Keble Road, Oxford OX1 3RH, UK*
[5]*Space Telescope Science Institute, 3700 San Martin Drive, Baltimore, MD 21218, USA*
[6]*Kavli Institute for Astronomy and Astrophysics, Peking University, Beijing 100871, People's Republic of China*
[7]*Physics and Astronomy Department, Johns Hopkins University, Baltimore, MD 21218, USA*
[8]*Department of Astronomy, Tsinghua University, Beijing 100084, China*
[9]*Department of Physics and Astronomy, FI-20014 University of Turku, Finland*
[10]*School of Sciences, European University Cyprus, Diogenes Street, Engomi, 1516 Nicosia, Cyprus*
[11]*National Astronomical Observatory of Japan, National Institutes of Natural Sciences, 2-21-1 Osawa, Mitaka, Tokyo 181-8588, Japan*
[12]*Graduate Institute for Advanced Studies, SOKENDAI, 2-21-1 Osawa, Mitaka, Tokyo 181-8588, Japan*
[13]*School of Physics and Astronomy, Monash University, Clayton, Victoria 3800, Australia*
[14]*Kavli Institute for Cosmology, University of Cambridge, Madingley Road, Cambridge CB3 0HA, UK*
[15]*Cavendish Laboratory, University of Cambridge, 19 JJ Thomson Avenue, Cambridge CB3 0HE, UK*
[16]*Department of Astronomy and Astrophysics, University of California, Santa Cruz, 1156 High Street, Santa Cruz CA 96054, USA*
[17]*NSF's National Optical-Infrared Astronomy Research Laboratory, 950 North Cherry Ave, Tucson, AZ 85719, USA*
[18]*Astrophysics Research Center of the Open University (ARCO), The Open University of Israel, Ra'anana 4353701, Israel*

ABSTRACT

The *James Webb Space Telescope* (*JWST*) discovered 79 transients out to $z \sim 4.8$ through the JADES Transient Survey (JTS), but the JTS did not find any $z > 5$ transients. Here, we present the first photometric evidence of a $z > 5$ transient/variable source with *JWST*. The source, AT 2023adya, resides in a $z_{\rm spec} = 5.274$ galaxy in GOODS-N, which dimmed from $m_{\rm F356W} = 26.05 \pm 0.02$ mag to 26.24 ± 0.02 mag in the rest-frame optical over approximately two rest-frame months, producing a clear residual signal in the difference image ($m_{\rm F356W} = 28.01 \pm 0.17$ mag; $\rm SN_{var} = 6.09$) at the galaxy center. Shorter-wavelength bands (F090W/F115W) show no rest-frame ultraviolet brightness change. Based on its rest-frame V-band absolute magnitude of $\rm M_V = -18.48$ mag, AT 2023adya could be any core-collapse supernova (SN) subtype or an SN Ia. However, due to low SN Ia rates at high redshift, the SN Ia scenario is unlikely. Alternatively, AT 2023adya may be a variable active galactic nucleus (AGN). However, the JWST NIRCam/Grism spectrum shows no broad Hα emission line (FWHM $= 130 \pm 26$ km s^{-1}), disfavoring the variable AGN scenario. It is also unlikely that AT 2023adya is a tidal disruption event (TDE) because the TDE models matching the observed brightness changes have low event rates. Although it is not possible to determine AT 2023adya's nature based on the two-epoch single-band photometry alone, this discovery indicates that *JWST* can push the frontier of transient/variable science past $z = 5$ and towards the epoch of reionization.

Corresponding author: Christa DeCoursey
cndecoursey@arizona.edu

Keywords: supernovae: general; galaxies: active

1. INTRODUCTION

With the launch of the *James Webb Space Telescope* (*JWST*), the redshift frontier of transient and variable science has extended far beyond the $z \sim 2$ *Hubble Space Telescope* (*HST*) frontier. The high-redshift ($z \geq 2$) transient and variable sources discovered with *JWST* thus far include Type Ia supernovae (SNe Ia; the thermonuclear explosions of white dwarfs), core-collapse (CC) SNe (explosions of $\geq 8 M_{\odot}$ stars), and active galactic nuclei (AGN).

Building a sample of high-redshift SNe Ia can provide useful constraints on SN Ia systematics (Riess & Livio 2006), including whether they are truly similar to low-redshift SNe Ia and can act as standard candles (Pierel et al. 2024a, 2025). This has implications especially for cosmology constraints achieved at higher redshifts, such as the possibility of an evolving dark energy equation of state parameter, w (Adame et al. 2025). CCSNe, on the other hand, closely trace the instantaneous star formation rate and thus provide an independent view of the cosmic star formation rate density. Observed CCSN rates can be compared to those expected from the cosmic star formation rate density to provide constraints on missing CCSN fractions, the progenitor mass range of CCSNe, and the potential scenario of an evolving IMF (Dahlen et al. 2012; Strolger et al. 2015). Additionally, there is evidence that CCSN explosion energies evolve with redshift (Coulter et al. 2025; Moriya et al. 2025). Building a larger sample of high-redshift CCSNe will generate better constraints on how high-redshift CCSNe differ from local CCSNe.

The *JWST* Advanced Deep Extragalactic Survey (JADES) program obtained two epochs of deep (∼30 mag) *JWST* near-infrared camera (NIRCam) images of the Great Observatories Origins Deep Survey South (GOODS-S) field, separated by one observer-frame year (Eisenstein et al. 2023). The JADES Transient Survey (JTS) discovered 38 supernovae (SNe) at $z > 2$, and the highest-redshift SN in the JTS sample is associated with a $z_{\rm phot} = 4.82$ host (DeCoursey et al. 2025). This sample includes an SN Ia at $z = 2.9$ (Pierel et al. 2024a), a Type Ic broad line (Ic-BL) SN at $z = 2.83$ (Siebert et al. 2024), and a likely Type IIP SN at $z = 3.61$ (Coulter et al. 2025). Moriya et al. (2025) explores the properties of the robustly-classified Type II SNe in the JTS sample, three of which are at $z > 2$. Additionally, within the COSMOS-Web SN survey, an SN Ia has been discovered at $z = 2.15$ (Pierel et al. 2025). There have also been multiple serendipitous SN discoveries with *JWST* (e.g. Yan et al. 2023), including multiply-lensed SNe Ia at $z = 1.78$ (Frye et al. 2024; Pierel et al. 2024b; Pascale et al. 2025) and $z = 1.95$ (Pierel et al. 2024c).

We conducted a systematic transient and variable search in the GOODS-North field with two sets of overlapping F090W, F115W, and F356W *JWST*/NIRCam imaging, separated by one observer-frame year (DeCoursey et al. 2024). This search yielded a sample of 39 transient and variable sources, one of which is AT 2023adya. AT 2023adya is associated with a $z_{\rm spec} = 5.274$ host galaxy (Sun et al. 2024), making it the highest-redshift transient/variable source showing a photometric change in brightness discovered thus far with *JWST*. We explore the types of transient or variable sources that may explain AT 2023adya, which include CCSNe, SNe Ia, variable AGN, and tidal disruption events (TDEs).

In Section 2, we describe the NIRCam observations covering AT 2023adya. Section 3 explains how we discovered AT 2023adya and presents the photometric measurements of AT 2023adya. We describe AT 2023adya's host and step through the possible sources of AT 2023adya's transient or variable nature in Section 4, and we summarize our findings in Section 5. Throughout this paper, we express magnitudes using the AB system (Oke & Gunn 1983) and adopt a flat ΛCDM cosmology with the following parameters: $H_0 = 70$ km s^{-1} Mpc^{-1}, $\Omega_\Lambda = 0.7$, and $\Omega_m = 0.3$.

2. DATA

2.1. *NIRCam Imaging*

The JADES program (program ID: 1181; PI: Eisenstein) obtained 9-band *JWST*/NIRCam imaging of GOODS-N on UT 2023 February 3, using 4 short-wavelength (SW) wide-band filters (F090W, F115W, F150W, F200W), 3 long-wavelength (LW) wide-band filters (F277W, F356W, F444W), and 2 LW medium-band filters (F335M, F410M). The JADES observing strategy is described in detail in Eisenstein et al. (2023).

Approximately one observer-frame year later on UT 2024 February 12–18, the Complete NIRCam Grism Redshift Survey (CONGRESS) program (program ID: 3577; PI: Egami) obtained 3-band *JWST*/NIRCam imaging of GOODS-N, using two SW wide-band filters (F090W, F115W) and one LW wide-band filter (F356W) (Egami et al. 2023). Rieke et al. (2023) pro-

* NASA Einstein Fellow

vides a detailed description of the data processing procedure for JADES NIRCam observations of GOODS-S. Similar data processing procedures were applied to the JADES GOODS-N NIRCam observations as well as the CONGRESS NIRCam observations (F. Sun et al. in preparation).

We focus our analysis on the overlapping region in GOODS-N ($\sim$38 arcmin^2) between the F090W, F115W, and F356W JADES and CONGRESS images. Each image was mosaicked into the same pixel grid, with the F356W images resampled from their $0\farcs06$/pixel native pixel scale to a $0\farcs03$/pixel scale. The JADES images are hereafter referred to as Epoch1, and the CONGRESS images are hereafter referred to as Epoch2.

2.2. *NIRCam/Grism Spectroscopy*

In addition to NIRCam imaging observations, CONGRESS simultaneously obtained $\sim$2-hr NIRCam/Grism Wide Field Slitless Spectroscopy (WFSS) observations of GOODS-N using the F356W filter. Previously, the First Reionization Epoch Spectroscopically Complete Observations (FRESCO) program (program ID: 1895; PI: Oesch) obtained $\sim$2-hr NIRCam/Grism WFSS observations of GOODS-N using the F444W filter on UT 2023 February 11–13 along with F444W, F182M, and F210M NIRCam imaging observations (Oesch et al. 2023). The spectral resolution of the NIRCam WFSS mode is R $\sim$ 1600 at 2.4–5.0 μm.

NIRCam grism data processing was detailed by Sun et al. (2024) following the public codes and calibrations[1] made available by Sun et al. (2023), including latest updates on tracing and wavelength calibration based on *JWST* Cycle-1 and 2 data.

3. RESULTS

3.1. *AT 2023adya Discovery*

To search for transient and variable sources between Epoch1 and Epoch2, we created difference images for each filter by subtracting the Epoch2 data from the Epoch1 data. In addition to visually inspecting the difference images for point-like emission, we used `DAOSTarFinder` to search for evidence of transient/variable sources in each of the difference images (Stetson 1987). We visually inspected the `DAOStarFinder` transient and variable candidates to remove contaminants such as noise spikes and diffraction spikes from the sample. This resulted in a sample of 39 transient and variable sources, which was reported to the Transient Name Server (TNS; DeCoursey et al. 2024). This sample includes AT 2023adya, positioned at (189°.12003, 62°.23867), which is exceptional because its host resides at $z_{\rm spec} = 5.274$ (Sun et al. 2024). Figure 1 shows AT 2023adya in Epoch1, Epoch2, and the Epoch1-Epoch2 difference images in the F090W, F115W, and F356W filters.

3.2. *Photometry*

We performed aperture photometry using `astropy photutils` (Bradley et al. 2024) on the difference image for each filter at AT 2023adya's position. We used an $r = 0\farcs2$ circular aperture on the difference images with appropriate aperture corrections, and we used an $r = 0\farcs4$–$0\farcs6$ annulus for sky subtraction. To measure flux uncertainty, we randomly placed $r = 0\farcs2$ circular apertures in the background and calculated the standard deviation of the background flux. Refer to the third row of Table 1 for the photometry measured from the difference images. We do not detect AT 2023adya in the F090W or F115W difference images, and hence $m_{\rm F090W} > 28.4$ mag and $m_{\rm F115W} > 28.7$ mag, which are 2σ upper limits. However, the difference image photometry for F356W yields $m_{\rm F356W} = 28.01 \pm 0.17$ mag. We list the rest-frame wavelengths at $z = 5.274$ associated with each filter in the bottom row of Table 1.

To verify that the F356W difference image emission at AT 2023adya's position is real and not a subtraction artifact, we performed aperture photometry at AT 2023adya's position in the Epoch1 and Epoch2 science images in each filter and measured the brightness variation of the whole galaxy. The two epochs of science image photometry are listed in the top two rows of Table 1. The difference between the F356W Epoch1 and Epoch2 science image photometry yields nearly the exact same value as the photometry measured from the difference image ($m_{\rm F356W} = 28.04 \pm 0.14$ mag), demonstrating that the F356W variability is real and not a subtraction artifact. AT 2023adya and its host were $\sim$19% brighter in Epoch1 than Epoch2. We also processed two epochs of imaging data by bootstrapping the NIRCam exposures that cover the position of AT 2023adya, produced multiple mosaicked images at both epochs and performed aperture photometry. Our bootstrapping test validates the F356W variability, which is not an artifact due to certain bad exposures.

Additionally, we computed the signal-to-noise ratio of variability (SN$_{\rm var}$) of the science image photometry using the following equation:

$$\mathrm{SN_{var}} = \frac{|\mathrm{flux_{Epoch1}} - \mathrm{flux_{Epoch2}}|}{\sqrt{\sigma^2_{\rm flux,Epoch1} + \sigma^2_{\rm flux,Epoch2}}}, \quad (1)$$

[1] https://github.com/fengwusun/nircam_grism

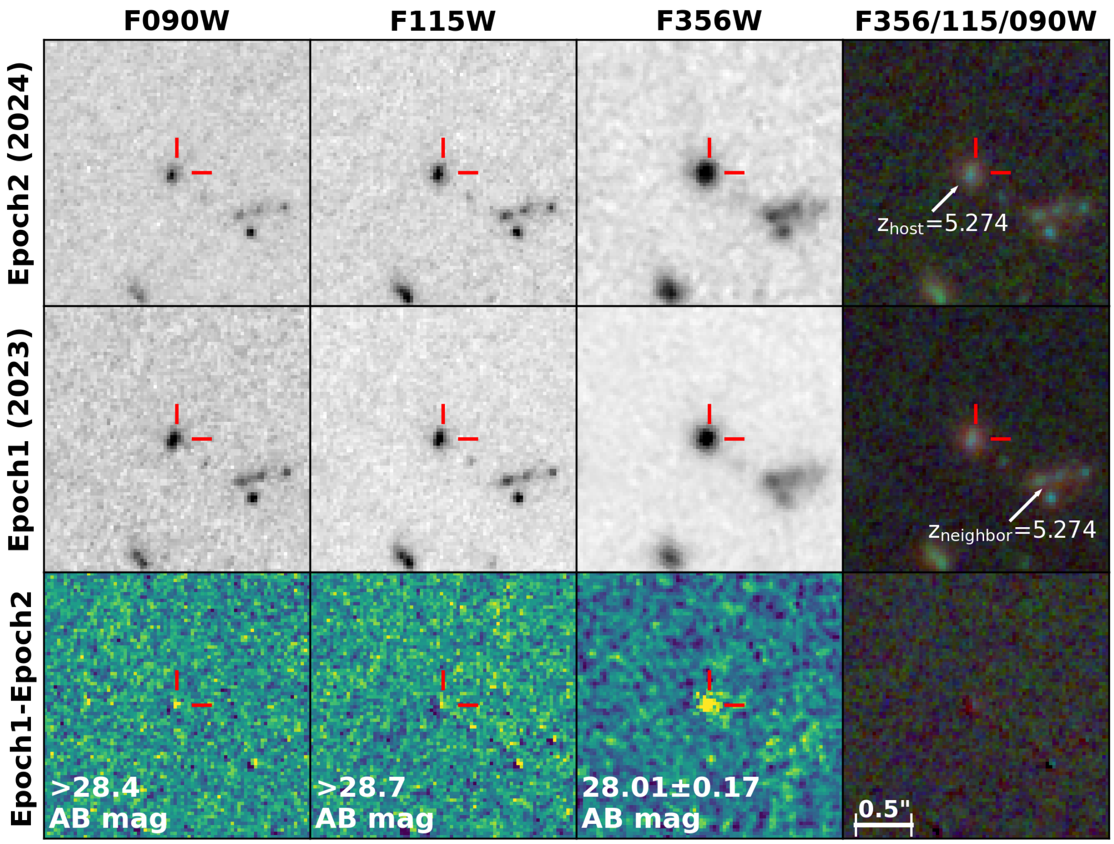

Figure 1. NIRCam images of AT 2023adya, with red crosshairs indicating AT 2023adya's position. *Top*: The Epoch2 (CONGRESS; 2024) F090W, F115W, and F356W NIRCam images. The right-most panel shows the F356W/F115W/F090W Epoch2 red-green-blue (RGB) image, with AT2023adya's host labeled. In these Epoch2 images, AT 2023adya has either faded or disappeared. *Middle*: The Epoch1 (JADES; 2023) F090W, F115W, and F356W NIRCam images (and F356W/F115W/F090W RGB image) of AT 2023adya. AT 2023adya is present in the F356W image, although its emission is blended with its host's emission. The host's companion is labeled in the RGB image. *Bottom*: The Epoch1-Epoch2 F090W, F115W, and F356W difference images (and F356W/F115W/F090W RGB difference image) showing AT 2023adya's change in brightness. There is clearly emission in the F356W difference image, indicating a change in brightness, but there is no emission in the F090W or F115W difference images.

where $\sigma_{\rm flux}$ is the flux uncertainty. The $\rm SN_{var}$ for F090W, F115W and F356W are <0.80, <0.92, and 6.09, respectively, further indicating that AT 2023adya exhibits a change in F356W brightness but does not exhibit a change in F090W or F115W brightness.

3.3. *AT 2023adya's Position and Host*

AT 2023adya was discovered at (189.°12003, 62.°23867) in GOODS-N and belongs to host galaxy JADES–GN+189.12004+62.23867. The host resides at $z_{\rm spec} = 5.274$ (Sun et al. 2024, the redshift is updated based on improved calibrations), measured unambiguously from an Hα emission line in the FRESCO F444W NIRCam/grism spectrum and an [O III] λ5008 emission line in the CONGRESS F356W NIRCam/grism spectrum. Sun et al. (2024) measured AT 2024adya's host to be centered at (189.°12004, +62.°23867), which is only ∼0.″02 (∼0.10 kpc) away from AT 2023adya's position. We re-measured the host centroid using the Epoch2 F356W image since Sun et al. (2024) measured the centroid using the AT 2023adya-contaminated images, but we find a negligible difference in the Epoch2 host centroid. Hence, we use the measurement from Sun et al. (2024) as the host centroid. The angular separation between AT 2023adya and its host's center is ∼1/3 of a native LW pixel, and thus AT 2023adya can be considered coincident with the host's center within the uncertainty, as shown in Figure 1.

Although there is 9-band *JWST*/NIRCam imaging from Epoch1, we do not perform host galaxy SED fitting because those images are contaminated with AT 2023adya, and thus the derived parameters from the SED fit may be unreliable. Epoch2 has only three *JWST*/NIRCam filters which is insufficient to produce a reliable SED fit.

Table 1. NIRCam Photometry

	F090W	F115W	F356W
Epoch1	26.54±0.05	26.51±0.04	26.05±0.02
Epoch2	26.48±0.06	26.45±0.05	26.24±0.02
Epoch1−Epoch2	>28.4 (2σ)	>28.7 (2σ)	28.01±0.17
SN_{var}	<0.80	<0.92	6.09
λ_{rest}	144nm	183nm	567 nm

NOTE—The F356W magnitude reported for AT 2023adya on TNS is slightly fainter ($m_{F356W} = 28.27 \pm 0.09$) due to the use of an 0.″1 aperture, which failed to capture all of AT 2023adya's emission.

4. DISCUSSION

Because we only detect a source brightness change in one filter between two imaging epochs, we cannot conclusively determine AT 2023adya's origin. However, we examine various possibilities, including an SN explosion, merger-induced AGN variability, and a TDE.

4.1. *Supernova*

We explore a variety of SN subtypes at $z = 5.274$ to determine which SN subtypes can mimic AT 2023adya's F356W magnitude. At $z = 5.274$, $m_{F356W} = 28.01$ mag translates to a rest-frame 567 nm (approximately V-band) absolute magnitude of $M_V = -18.48$ mag. This absolute magnitude provides constraints on the types of SNe that may explain AT 2023adya.

We plot the volume-limited Gaussian distribution of peak absolute B-band magnitude for SNe Ib, Ic, IIP, IIL, IIn, and Ia in Figure 2 (Richardson et al. 2014). The Richardson et al. (2014) absolute B-band magnitudes primarily come from the low-redshift Asiago Supernova Catalog sample. We will treat AT 2023adya's $M_V = -18.48$ mag as a lower limit on brightness compared to the peak B-band distributions because (1) it is unlikely that we observed AT 2023adya at its peak V-band absolute magnitude, and (2) it is possible that AT 2023adya is still present in Epoch2, which would cause the difference image photometry to underestimate AT 2023adya's absolute brightness.

This interpretation implies that only SNe which have absolute B-band magnitudes equal to or brighter than $M_V = -18.48$ mag can explain AT 2023adya. However, it should be noted that SNe Ib/c peak brighter in the rest-frame V-band than B-band (Woosley et al. 2021; Jin et al. 2023), and SNe II and SNe Ia tend to peak at similar rest-frame V-band and B-band absolute magnitudes or slightly brighter in the rest-frame V-band than B-band (Ashall et al. 2016; de Jaeger et al. 2019; Jin et al. 2023; Anderson et al. 2024). Therefore, treating AT 2023adya's absolute V-band magnitude as a lower limit on brightness relative to the peak B-band absolute magnitude distributions will result in conservative conclusions on the SN subtypes that are compatible with AT 2023adya, since the V-band peak absolute magnitude distributions are similar or brighter than those of the B-band.

As shown in Figure 2, SNe Ib, Ic, and IIL with typical peak B-band absolute magnitudes are too faint to explain AT 2023adya, but the bright tails of these CCSN subtypes are sufficiently luminous. Both typical and bright SNe IIn and Ia are bright enough to explain AT 2023adya.

4.1.1. *SN IIP*

At $z = 5.274$, F115W approximately corresponds to the rest-frame near-UV (NUV; ∼183nm) and F356W approximately corresponds to the rest-frame V-band. As seen in Figure 2, only the brightest SNe IIP are sufficiently luminous to explain AT 2023adya. No typical low-redshift SN IIP is comparable to AT 2023adya.

However, we can compare AT 2023adya to SN 2009kf, a $z = 0.182$ SN IIP that was bright not only in V-band ($M_{V,peak} \approx -19.45$ mag) but also incredibly bright in the NUV ($M_{NUV,peak} \approx -21.5 \pm 0.5$ mag). Dense circumstellar medium interaction caused the unusual NUV brightness (Botticella et al. 2010; Moriya et al. 2011).

At SN 2009kf's redshift of $z = 0.182$, the effective *Galaxy Evolution Explorer* (*GALEX*) NUV wavelength corresponds to rest-frame ∼195nm and thus probes a similar rest-frame wavelength as AT 2023adya's F115W photometric non-detection. F115W's limiting magnitude of $m_{F115W} \leq 28.7$ mag corresonds to $M_{NUV} \lesssim -17.8$ mag at $z = 5.274$, and if AT 2023adya is similar to SN 2009kf, it would have peaked around $M_{NUV} = -21.5$ mag, well above the detection limit. In other words, if AT 2023adya is SN 2009kf-like, it probably would have been detected in F115W. However, we cannot rule out the possibility of dust-extinction causing the NUV non-detection. We are unfortunately unable to

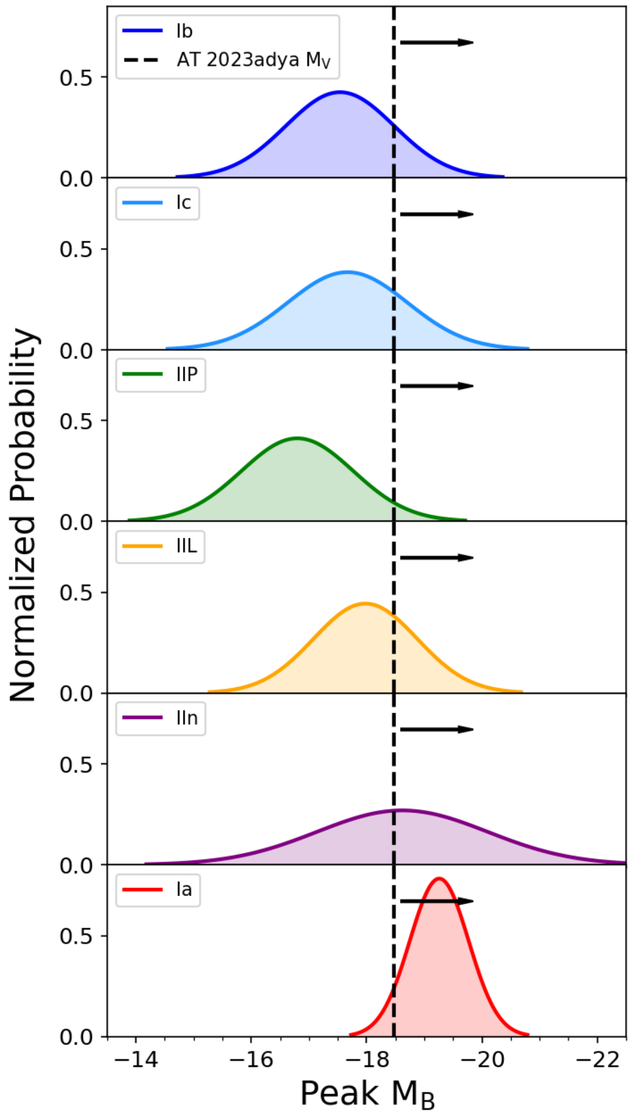

Figure 2. The Gaussian distributions of peak absolute B-band magnitudes from Richardson et al. (2014) for SNe Ib (dark blue), Ic (light blue), IIP (green), IIL (orange), IIn (purple), and Ia (red). The vertical black dashed line shows AT 2023adya's rest-frame 567 nm (approximately V-band) absolute magnitude. It is unlikely that AT 2023adya was exactly at its V-band peak in Epoch1 and AT 2023adya may still be present in Epoch2, so AT 2023adya's V-band absolute magnitude can be treated as a lower limit on brightness relative to the peak absolute B-band magnitude distributions (hence the black arrows).

provide constraints on potential dust extinction because the 9-band Epoch1 host SED is contaminated with AT 2023adya and thus provides unreliable host characteristics.

We are thus unable to rule out the possibility that AT 2023adya is a luminous, potentially dust-extincted SN IIP. The high-redshift SNe II from the JTS have tentatively shown evolution toward higher luminosities and hence toward higher explosion energies (Coulter et al. 2025; Moriya et al. 2025), highlighting the possibility that AT 2023adya is a luminous SN IIP.

4.1.2. *SN Ia*

Additionally, most SNe Ia, including underluminous 1991bg-like SNe Ia (Filippenko et al. 1992; Graur 2024), are sufficiently bright to explain AT 2023adya. Only the least luminous SNe Ia are incompatible with AT 2023adya's F356W magnitude, as shown in the bottom panel of Figure 2.

The SN Ia delay-time distribution (DTD) is the distribution of elapsed time between a hypothetical instantaneous burst of star formation and an SN Ia explosion. The observed DTD ranges from ∼10 Myr to ∼10 Gyr (Maoz et al. 2012; Graur & Maoz 2013; Maoz & Graur 2017; Liu et al. 2023). Assuming that AT 2023adya is an SN Ia and the progenitor formed at $z \sim 10$, the delay-time would be ∼0.6 Gyr, which is within the expected range of DTDs. It is therefore physically possible that AT 2023adya is an SN Ia.

However, due to the decline of SN Ia rates at high redshift, it is unlikely that AT 2023adya is an SN Ia. Rodney et al. (2014) computed volumetric SN Ia rates out to $z \sim 2.5$ based on *HST* observations. Their Figure 9 hints at a decrease in the SN Ia rate beyond $z \sim 2$, though the error bars are large. Palicio et al. (2024) computed theoretical SN Ia rates by convolving various observed cosmic star formation rates with various DTDs. The theoretical SN Ia rates shown in their Figure 3 show a strong decline beyond $z \sim 2$ where the longer delay times become unphysical. Therefore, although the photometry we measure matches what we would expect for an SN Ia, the sheer number of CCSNe we would expect at this redshift compared to SNe Ia leads us to believe AT 2023adya is more likely of the former class.

4.1.3. *Exotic SNe*

To explore the superluminous SN (SLSN) possibility, we take the SLSN-I light curve model from Moriya et al. (2022) and redshift it to $z = 5.274$. We find that this SLSN model is compatible with AT 2023adya's observational signatures if it is post-peak, as the F115W light curve will be below the detection threshold while the F356W light curve will be well above the detection threshold. However, given the rarity of SLSNe and that AT 2023adya is compatible with normal SNe, it is unlikely that AT 2023adya is an SLSN.

We also explore a variety of pair-instability SN (PISN) model light curves from Kasen et al. (2011) and found that the bare helium core and hydrogenic red supergiant models at a variety of masses can reproduce the F356W detection and lack of F090W and F115W detections at $z = 5.274$. However, again given the rarity of PISNe and that AT 2023adya is compatible with many normal SNe, there is no compelling evidence that AT 2023adya is a PISN.

We cannot fully explore the fast blue optical transient (FBOT) possibility because we do not have rest-frame r-band or g-band measurements (selection generally requires g–$r \lesssim$-0.2; Drout et al. 2014), and we do not have the proper cadence to determine the rise and fall time (selection generally requires that the duration above the light curve half-maximum to be 1 day $< t_{1/2} < 12$ days; Ho et al. 2023). However, Drout et al. (2014) estimates a volumetric FBOT rate of 4–7% of the CCSN rate at $z \sim 0.2$ (Botticella et al. 2008), and Ho et al. (2023) estimates that the luminous FBOT (LFBOT) rate is $\lesssim 0.1$% of the local CCSN rate, making it unlikely that AT 2023adya is an FBOT or LFBOT.

4.2. *Active Galactic Nucleus*

Optical variability is a common selection technique to identify AGN (Klesman & Sarajedini 2007; Trevese et al. 2008; Villforth et al. 2010; De Cicco et al. 2015; García-González et al. 2015; Yuk et al. 2022), as many Type 1 AGN exhibit variability on timescales ranging from hours to years (Ulrich et al. 1997; Vanden Berk et al. 2004; Sesar et al. 2007; Hickox et al. 2014). Type 1 AGN exhibit a broad Hα emission line (≥ 1000 km/s) that cannot be attributed to normal star-forming galaxy activity. Under the widely-accepted assumption that this broad Hα emission is connected to AGN activity, the AGN broad line region (BLR) generates the broad Hα emission.

There have been numerous searches for AGN variability with *JWST*, especially with regards to Type 1 AGN and "Little Red Dots" (LRDs: red, compact, high-redshift objects which are thought to be dusty AGN; Kokubo & Harikane 2024; Zhang et al. 2024). Photometric variability has generally not yet been observed for Type 1 AGN and LRDs with the limited amount of *JWST* data available so far. However, there is evidence of spectral variability in multiply-imaged LRD A2744-QSO1 at $z = 7.04$ (Ji et al. 2025; Furtak et al. 2025). The JTS reports seven variable AGN candidates, none of which are LRDs or have been identified as Type 1 AGN (DeCoursey et al. 2025).

Theoretical models presented in Hopkins et al. (2006), Somerville et al. (2008), and Hickox et al. (2014) indicate that mergers are a primary mechanism for driving AGN activity. AT 2023adya's host is a member of a high-confidence merger pair (~80% close pair probability; Puskás et al. 2025), residing only ~5.2 kpc from JADES-GN-189.11960+62.23855 ($z_{\rm spec} = 5.274$; Sun et al. 2024), and is also part of overdensity JADES–GN–OD–5.269 (Helton et al. 2024). This suggests that AT 2023adya could result from merger-induced AGN activity.

AT 2023adya's host has not been previously identified as an AGN candidate (Lyu et al. 2022, 2024), but this is not unexpected due to its relatively high redshift and limited wavelength coverage. A broad Hα emission line generated within the AGN BLR is a Type 1 AGN signature. As shown in the left side of Figure 3, we fit the host's Hα emission with a single Gaussian component considering the grism line spread function calibrated by Sun, F. et al. (in preparation), and it does not exhibit broad Hα emission. Rather, the FWHM of the Hα line is only 130±26 km/s (the Hα line flux is $7.1 \pm 0.4 \times 10^{-18}$ erg s^{-1} cm^{-2}). This F444W NIRCam/Grism spectrum showing narrow Hα was taken approximately one observer-frame week after the Epoch1 NIRCam imaging. The right side of Figure 3 shows a single-component fit to the host's [O III] λ5008 emission line, which has a FWHM of 186±30 km s^{-1} and a line flux of $1.32 \pm 0.07 \times 10^{-17}$ erg s^{-1} cm^{-2}. This F356W NIRCam/Grism spectrum was taken at the time of Epoch2.

López-Navas et al. (2023) analyzed the Zwicky Transient Facility light curves of ~50% of the AGN from Sloan Digital Sky Survey (SDSS) data release 16 and found that Type 2 AGN show negligible optical variations, and the Type 2 AGN that do show optical variations are likely misclassified Type 1 AGN or changing-look/changing-state AGN. Barth et al. (2014) searched for optical g-band variability among the luminous Type 2 AGN in SDSS Stripe82 and similarly found that the majority of Type 2 AGN do not exhibit optical variability, and most or all of the variable AGN in the Type 2 sample are likely Type 1 contaminants. The lack of a broad Hα component in AT 2023adya's host spectrum during Epoch1 means either (1) our view of the AGN BLR is blocked by dust (i.e., Type 2 AGN), or (2) if we have a direct view toward the galaxy center, the galaxy nucleus is not active. In either case, we would not expect to see 19% change in brightness over 2 rest-frame months, suggesting that AT 2023adya is not likely to arise from AGN activity. Although it is difficult to exclude the existence of a faint broad-line component based on the limited-depth NIRCam/Grism spectrum, a 19% brightness change would have made such a component visible in the spectrum.

4.3. *Tidal Disruption Event*

A TDE occurs when a supermassive black hole (SMBH) shreds apart a star that passes within its tidal

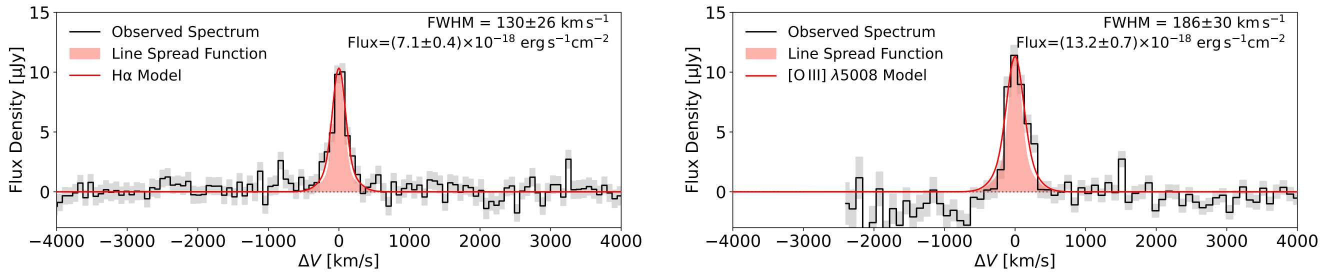

Figure 3. NIRCam grism spectra of the Hα (left; with FRESCO F444W) and [O III] λ5008 (right; with CONGRESS F356W) emission lines of AT 2023adya's host, shown as solid black lines with uncertainties in gray shades. Line spread functions (Sun, F. et al., in prep.) at line centroids are shown as shallow red shades, and best-fit Gaussian profiles convolved with the line spread functions are shown as the solid red lines. Both lines do not show hints of broad components. Note that the [O III] λ5008 line is at the blue edge of the F356W transmission and the continuum / background subtraction is not optimal.

radius, generating a luminous accretion flare (Rees 1988; Evans & Kochanek 1989; Ulmer 1999). TDEs are expected to be abundant at high redshifts, due to the high central stellar densities of high redshift galaxies and the slightly lower SMBH masses (Karmen et al. 2025). Inayoshi et al. (2024) find that deep *JWST* surveys can discover TDEs occurring in moderately obscured AGN (e.g., with typical attenuation levels of $A_{\rm V} \sim 3$ mag, as seen in LRDs) up to $z \approx 4$–7 even with small survey areas. These observations enable the exploration for the mass distribution of SMBHs at the low-mass end, where their abundance is sufficiently high for detection. Pfister et al. (2021) uses hydrodynamical simulations to show that the TDE rate can be enhanced at early cosmological times, and that TDEs could be a viable growth mechanism for massive black hole seeds. Additionally, Karmen et al. (2025) reports the discovery of a high-redshift TDE candidate in the COSMOS-Web field, identified using novel color and morphology selection criteria. This further suggests enhanced TDE rates at high-redshift relative to the local rate.

Despite these predictions, however, it is difficult to explain AT 2023adya as a TDE. TDEs are extremely UV-bright, and yet AT 2023adya exhibits no change in rest-frame UV brightness. Therefore, if AT 2023adya is a TDE, it must be embedded in the dusty nucleus of a galaxy (e.g. Masterson et al. 2024). Although it is possible to produce a dust-obscured TDE SED that is red enough to explain the F356W detection and the F090W/F115W non-detections of AT 2023adya, producing the observed F356W magnitude of $\sim$28 mag for a $z = 5$ TDE is not straightforward. For example, the $z = 5$ dust-obscured TDE SED model of Inayoshi et al. (2024) with $\rm M_{SMBH} = 10^5\ M_\odot$ and $A_{\rm V} \gtrsim 3$ mag in their Figure 8 can reproduce the required SED color and match the high detection rate inferred by the small survey area of ~ 38 arcmin^2 (corresponding to ~ 100 deg^{-2}yr^{-1}, see their Figure 5). However, this model remains $\sim$1 mag fainter ($\sim$29 mag) than AT 2023adya's F356W detection even at peak brightness. While a more luminous TDE model with a luminosity exceeding $\sim 10^{45}$ erg s^{-1} (observationally rarer in the nearby universe; see Table 1 of Gezari 2021) or a more massive SMBH could match the observed brightness, both options would imply a lower event rate and space density, making detection within our survey less likely (e.g., Inayoshi et al. 2024).

5. CONCLUSION

We discovered AT 2023adya by differencing F356W NIRCam imaging in GOODS-N taken one observer-frame year apart by the JADES and CONGRESS programs. AT 2023adya is thus far the highest-redshift transient/variable source showing a change in photometric brightness discovered with *JWST*, residing in a $z_{\rm spec} = 5.274$ galaxy which faded from $m_{\rm F356W} = 26.05 \pm 0.02$ mag to 26.24 ± 0.02 mag (+0.19 mag) over approximately two rest-frame months. The F356W difference image shows a clear residual signal ($m_{\rm F356W} = 28.01 \pm 0.17$ mag). AT 2023adya does not, however, exhibit rest-frame UV variability in the F090W or F115W filters. While we cannot determine the true nature of AT 2023adya, we explore various sources that may create the observed brightness change, including an SN explosion, merger-induced AGN activity, and a TDE.

- Any CCSN subtype can explain AT 2023adya's F356W magnitude, although each CCSN subtype except for SNe IIn would need to be brighter than average. Although we cannot exclude the possibility that AT 2023adya is an SN Ia based on its observed brightness, the bright CCSN scenario is more likely because CCSN rates are expected to dominate over SN Ia rates at high redshift.

- AT 2023adya's host is a member of a high-confidence galaxy merger pair (Puskás et al. 2025), indicating that AT 2023adya may be the signature of merger-induced AGN activity. However, we did not observe broad Hα emission in AT 2023adya's F444W NIRCam/grism spectrum one observer-frame week after the Epoch1 imaging, meaning that AT 2023adya is unlikely to be a Type 1 AGN. This disfavors the AGN scenario, as Type 2 AGN exhibit negligible variability. NIRCam/Grism's limited depth does make it difficult to exclude the existence of a faint broad-line component in the F444W spectrum, but a 19% brightness change would have made such a component visible in the spectrum.

- It is unlikely that AT 2023adya is a TDE due to the low event rate of TDEs matching the observed photometry (i.e., with sufficient dust to obscure the rest-frame UV emission and sufficient optical luminosity to match the F356W photometry).

Although we cannot determine AT 2023adya's true nature with the available data, this discovery is significant because it represents the first piece of photometric evidence that *JWST* can robustly detect transient/variable sources at $z > 5$. It is notable that the JTS discovered no such sources at $z > 5$ in GOODS-S. Had a source similar to AT 2023adya been in the JADES Deep Field within GOODS-S, the JTS selection criteria likely would have identified it. The lack of $z > 5$ transient and variable sources in the JTS sample indicates the rarity of discovering such sources at high redshift when the baseline between observations is only one observer-frame year. To continue building the $z > 5$ transient and variable source sample, which may include exotic sources such as Population III SNe, we will conduct multi-epoch multi-filter *JWST* observations with baselines longer than one observer-frame year through Cycle-4 *JWST* Program 8060 (PI: Egami).

Acknowledgements

This work is based on observations made with the NASA/ESA/CSA James Webb Space Telescope. The data were obtained from the Mikulski Archive for Space Telescopes at the Space Telescope Science Institute, which is operated by the Association of Universities for Research in Astronomy, Inc., under NASA contract NAS 5-03127 for JWST. These observations are associated with program #1181, 1895 and 3577. The specific JWST observations analyzed can be accessed via doi:10.17909/8tdj-8n28 and doi:10.17909/6rfk-6s81 . Support for program #3577 was provided by NASA through a grant from the Space Telescope Science Institute, which is operated by the Association of Universities for Research in Astronomy, Inc., under NASA contract NAS 5-03127. The authors acknowledge the FRESCO team for developing their observing program with a zero-exclusive-access period.

A.J.B. acknowledges funding from the "FirstGalaxies" Advanced Grant from the European Research Council (ERC) under the European Union's Horizon 2020 research and innovation program (Grant agreement No. 789056). K.I. acknowledges support from the National Natural Science Foundation of China (12073003, 12003003, 11721303, 11991052, and 11950410493) and the China Manned Space Project (CMS-CSST-2021-A04 and CMS-CSST-2021-A06). S.M. acknowledges support from the Research Council of Finland project 350458. D.P. acknowledges support by the Huo Family Foundation through a P.C. Ho PhD Studentship. E.E., B.D.J., G.R., and B.E.R. acknowledge support from the JWST/NIRCam contract to the University of Arizona NAS5-02015. B.E.R. also acknowledges support from the JWST Program 3215. S.T. acknowledges support by the Royal Society Research Grant G125142. The research of C.C.W. is supported by NOIRLab, which is managed by the Association of Universities for Research in Astronomy (AURA) under a cooperative agreement with the National Science Foundation. The authors acknowledge use of the lux supercomputer at UC Santa Cruz, funded by NSF MRI grant AST 1828315.

Facilities: *JWST*

Software: astropy (Astropy Collaboration et al. 2022), photutils (Bradley et al. 2024)

REFERENCES

Adame, A. G., Aguilar, J., Ahlen, S., et al. 2025, JCAP, 2025, 021, doi: 10.1088/1475-7516/2025/02/021

Anderson, J. P., Contreras, C., Stritzinger, M. D., et al. 2024, A&A, 692, A95, doi: 10.1051/0004-6361/202244401

Ashall, C., Mazzali, P., Sasdelli, M., & Prentice, S. J. 2016, MNRAS, 460, 3529, doi: 10.1093/mnras/stw1214

Astropy Collaboration, Price-Whelan, A. M., Lim, P. L., et al. 2022, ApJ, 935, 167

Barth, A. J., Voevodkin, A., Carson, D. J., & Woźniak, P. 2014, AJ, 147, 12, doi: 10.1088/0004-6256/147/1/12

Botticella, M. T., Riello, M., Cappellaro, E., et al. 2008, A&A, 479, 49, doi: 10.1051/0004-6361:20078011

Botticella, M. T., Trundle, C., Pastorello, A., et al. 2010, ApJL, 717, L52, doi: 10.1088/2041-8205/717/1/L52

Bradley, L., Sipőcz, B., Robitaille, T., et al. 2024, astropy/photutils: 1.12.0, 1.12.0, Zenodo

Coulter, D. A., Pierel, J. D. R., DeCoursey, C., et al. 2025, arXiv e-prints, arXiv:2501.05513, doi: 10.48550/arXiv.2501.05513

Dahlen, T., Strolger, L.-G., Riess, A. G., et al. 2012, ApJ, 757, 70, doi: 10.1088/0004-637X/757/1/70

De Cicco, D., Paolillo, M., Covone, G., et al. 2015, A&A, 574, A112, doi: 10.1051/0004-6361/201424906

de Jaeger, T., Zheng, W., Stahl, B. E., et al. 2019, MNRAS, 490, 2799, doi: 10.1093/mnras/stz2714

DeCoursey, C., Egami, E., Sun, F., et al. 2024, Transient Name Server AstroNote, 264, 1

DeCoursey, C., Egami, E., Pierel, J. D. R., et al. 2025, ApJ, 979, 250, doi: 10.3847/1538-4357/ad8fab

Drout, M. R., Chornock, R., Soderberg, A. M., et al. 2014, ApJ, 794, 23, doi: 10.1088/0004-637X/794/1/23

Egami, E., Sun, F., Alberts, S., et al. 2023, Complete NIRCam Grism Redshift Survey (CONGRESS), JWST Proposal. Cycle 2, ID. #3577

Eisenstein, D. J., Willott, C., Alberts, S., et al. 2023, arXiv e-prints, arXiv:2306.02465, doi: 10.48550/arXiv.2306.02465

Evans, C. R., & Kochanek, C. S. 1989, ApJL, 346, L13, doi: 10.1086/185567

Filippenko, A. V., Richmond, M. W., Branch, D., et al. 1992, AJ, 104, 1543, doi: 10.1086/116339

Frye, B. L., Pascale, M., Pierel, J., et al. 2024, ApJ, 961, 171, doi: 10.3847/1538-4357/ad1034

Furtak, L. J., Secunda, A. R., Greene, J. E., et al. 2025, arXiv e-prints, arXiv:2502.07875, doi: 10.48550/arXiv.2502.07875

García-González, J., Alonso-Herrero, A., Pérez-González, P. G., et al. 2015, MNRAS, 446, 3199, doi: 10.1093/mnras/stu2204

Gezari, S. 2021, ARA&A, 59, 21, doi: 10.1146/annurev-astro-111720-030029

Graur, O. 2024, MNRAS, 530, 4950, doi: 10.1093/mnras/stae949

Graur, O., & Maoz, D. 2013, MNRAS, 430, 1746, doi: 10.1093/mnras/sts718

Helton, J. M., Sun, F., Woodrum, C., et al. 2024, ApJ, 974, 41, doi: 10.3847/1538-4357/ad6867

Hickox, R. C., Mullaney, J. R., Alexander, D. M., et al. 2014, ApJ, 782, 9, doi: 10.1088/0004-637X/782/1/9

Ho, A. Y. Q., Perley, D. A., Gal-Yam, A., et al. 2023, ApJ, 949, 120, doi: 10.3847/1538-4357/acc533

Hopkins, P. F., Somerville, R. S., Hernquist, L., et al. 2006, ApJ, 652, 864, doi: 10.1086/508503

Inayoshi, K., Kashiyama, K., Li, W., et al. 2024, ApJ, 966, 164, doi: 10.3847/1538-4357/ad344c

Ji, X., Maiolino, R., Übler, H., et al. 2025, arXiv e-prints, arXiv:2501.13082, doi: 10.48550/arXiv.2501.13082

Jin, H., Yoon, S.-C., & Blinnikov, S. 2023, ApJ, 950, 44, doi: 10.3847/1538-4357/accf0d

Karmen, M., Gezari, S., Lambrides, E., et al. 2025, arXiv e-prints, arXiv:2504.13248. https://arxiv.org/abs/2504.13248

Kasen, D., Woosley, S. E., & Heger, A. 2011, ApJ, 734, 102, doi: 10.1088/0004-637X/734/2/102

Klesman, A., & Sarajedini, V. 2007, ApJ, 665, 225, doi: 10.1086/519442

Kokubo, M., & Harikane, Y. 2024, arXiv e-prints, arXiv:2407.04777, doi: 10.48550/arXiv.2407.04777

Liu, Z.-W., Röpke, F. K., & Han, Z. 2023, Research in Astronomy and Astrophysics, 23, 082001, doi: 10.1088/1674-4527/acd89e

López-Navas, E., Arévalo, P., Bernal, S., et al. 2023, MNRAS, 518, 1531, doi: 10.1093/mnras/stac3174

Lyu, J., Alberts, S., Rieke, G. H., & Rujopakarn, W. 2022, ApJ, 941, 191, doi: 10.3847/1538-4357/ac9e5d

Lyu, J., Alberts, S., Rieke, G. H., et al. 2024, ApJ, 966, 229, doi: 10.3847/1538-4357/ad3643

Maoz, D., & Graur, O. 2017, ApJ, 848, 25, doi: 10.3847/1538-4357/aa8b6e

Maoz, D., Mannucci, F., & Brandt, T. D. 2012, MNRAS, 426, 3282, doi: 10.1111/j.1365-2966.2012.21871.x

Masterson, M., De, K., Panagiotou, C., et al. 2024, ApJ, 961, 211, doi: 10.3847/1538-4357/ad18bb

Moriya, T., Tominaga, N., Blinnikov, S. I., Baklanov, P. V., & Sorokina, E. I. 2011, MNRAS, 415, 199, doi: 10.1111/j.1365-2966.2011.18689.x

Moriya, T. J., Quimby, R. M., & Robertson, B. E. 2022, ApJ, 925, 211, doi: 10.3847/1538-4357/ac415e

Moriya, T. J., Coulter, D. A., DeCoursey, C., et al. 2025, arXiv e-prints, arXiv:2501.08969, doi: 10.48550/arXiv.2501.08969

Oesch, P. A., Brammer, G., Naidu, R. P., et al. 2023, MNRAS, 525, 2864, doi: 10.1093/mnras/stad2411

Oke, J. B., & Gunn, J. E. 1983, ApJ, 266, 713, doi: 10.1086/160817

Palicio, P. A., Matteucci, F., Della Valle, M., & Spitoni, E. 2024, A&A, 689, A203, doi: 10.1051/0004-6361/202449740

Pascale, M., Frye, B. L., Pierel, J. D. R., et al. 2025, ApJ, 979, 13, doi: 10.3847/1538-4357/ad9928

Pfister, H., Dai, J. L., Volonteri, M., et al. 2021, MNRAS, 500, 3944, doi: 10.1093/mnras/staa3471

Pierel, J. D. R., Engesser, M., Coulter, D. A., et al. 2024a, ApJL, 971, L32, doi: 10.3847/2041-8213/ad6908

Pierel, J. D. R., Frye, B. L., Pascale, M., et al. 2024b, ApJ, 967, 50, doi: 10.3847/1538-4357/ad3c43

Pierel, J. D. R., Newman, A. B., Dhawan, S., et al. 2024c, ApJL, 967, L37, doi: 10.3847/2041-8213/ad4648

Pierel, J. D. R., Coulter, D. A., Siebert, M. R., et al. 2025, ApJL, 981, L9, doi: 10.3847/2041-8213/adb1d9

Puskás, D., Tacchella, S., Simmonds, C., et al. 2025, arXiv e-prints, arXiv:2502.01721, doi: 10.48550/arXiv.2502.01721

Rees, M. J. 1988, Nature, 333, 523, doi: 10.1038/333523a0

Richardson, D., Jenkins, III, R. L., Wright, J., & Maddox, L. 2014, AJ, 147, 118, doi: 10.1088/0004-6256/147/5/118

Rieke, M. J., Robertson, B., Tacchella, S., et al. 2023, ApJS, 269, 16

Riess, A. G., & Livio, M. 2006, ApJ, 648, 884, doi: 10.1086/504791

Rodney, S. A., Riess, A. G., Strolger, L.-G., et al. 2014, AJ, 148, 13, doi: 10.1088/0004-6256/148/1/13

Sesar, B., Ivezić, Ž., Lupton, R. H., et al. 2007, AJ, 134, 2236, doi: 10.1086/521819

Siebert, M. R., DeCoursey, C., Coulter, D. A., et al. 2024, ApJL, 972, L13, doi: 10.3847/2041-8213/ad6c32

Somerville, R. S., Hopkins, P. F., Cox, T. J., Robertson, B. E., & Hernquist, L. 2008, MNRAS, 391, 481, doi: 10.1111/j.1365-2966.2008.13805.x

Stetson, P. B. 1987, PASP, 99, 191

Strolger, L.-G., Dahlen, T., Rodney, S. A., et al. 2015, ApJ, 813, 93, doi: 10.1088/0004-637X/813/2/93

Sun, F., Egami, E., Pirzkal, N., et al. 2023, ApJ, 953, 53, doi: 10.3847/1538-4357/acd53c

Sun, F., Helton, J. M., Egami, E., et al. 2024, ApJ, 961, 69, doi: 10.3847/1538-4357/ad07e3

Trevese, D., Boutsia, K., Vagnetti, F., Cappellaro, E., & Puccetti, S. 2008, A&A, 488, 73, doi: 10.1051/0004-6361:200809884

Ulmer, A. 1999, ApJ, 514, 180, doi: 10.1086/306909

Ulrich, M.-H., Maraschi, L., & Urry, C. M. 1997, ARA&A, 35, 445, doi: 10.1146/annurev.astro.35.1.445

Vanden Berk, D. E., Wilhite, B. C., Kron, R. G., et al. 2004, ApJ, 601, 692, doi: 10.1086/380563

Villforth, C., Koekemoer, A. M., & Grogin, N. A. 2010, ApJ, 723, 737, doi: 10.1088/0004-637X/723/1/737

Woosley, S. E., Sukhbold, T., & Kasen, D. N. 2021, ApJ, 913, 145, doi: 10.3847/1538-4357/abf3be

Yan, H., Ma, Z., Sun, B., et al. 2023, ApJS, 269, 43, doi: 10.3847/1538-4365/ad0298

Yuk, H., Dai, X., Jayasinghe, T., et al. 2022, ApJ, 930, 110, doi: 10.3847/1538-4357/ac6423

Zhang, Z., Jiang, L., Liu, W., & Ho, L. C. 2024, arXiv e-prints, arXiv:2411.02729, doi: 10.48550/arXiv.2411.02729